

Bolometric light curves of supernovae and post-explosion magnetic fields

P. Ruiz-Lapuente ^{1,2}, and H. C. Spruit ²

Received _____; accepted _____

Running title: SNe light curves and magnetic fields

arXiv:astro-ph/9711248v1 20 Nov 1997

¹Department of Astronomy, University of Barcelona Martí i Franqués, 1 – E-08028
Barcelona, Spain

²Max-Planck-Institut für Astrophysik Karl-Schwarschild-Str. 1 – D-85740 Garching,
Germany

ABSTRACT

The various effects leading to diversity in the bolometric light curves of supernovae are examined: nucleosynthesis, kinematic differences, ejected mass, degree of mixing, and configuration and intensity of the magnetic field are discussed. In Type Ia supernovae, a departure in the bolometric light curve from the full-trapping decline of ^{56}Co can occur within the two and a half years after the explosion, depending on the evolutionary path followed by the WD during the accretion phase. If convection has developed in the WD core during the pre-supernova evolution, starting several thousand years before the explosion, a tangled magnetic field close to the equipartition value should have grown in the WD. Such an intense magnetic field would confine positrons where they originate from the ^{56}Co decays, and preclude a strong departure from the full-trapping decline, as the supernova expands. This situation is expected to occur in C+O Chandrasekhar WDs as opposed to edge-lit detonated sub-Chandrasekhar WDs. If the pre-explosion magnetic field of the WD is less intense than 10^{5-8}G , a lack of confinement of the positrons emitted in the ^{56}Co decay and a departure from full-trapping of their energy would occur. The time at which the departure takes place can provide estimates of the original magnetic field of the WD, its configuration, and also of the mass of the supernova ejecta. In SN 1991bg, the bolometric light curve suggests absence of a significant tangled magnetic field: its intensity is estimated to be lower than 10^3 G . Chandrasekhar-mass models do not reproduce the bolometric light curve of this supernova. For SN 1972E, on the contrary, there is evidence for a tangled configuration of the magnetic field and its light curve is well reproduced by a Chandrasekhar WD explosion. A comparison is made for the diagram of absolute magnitude and rate of decline in Type Ia supernovae coming from different explosion mechanisms. The effects

of mixing and ejected mass in the bolometric light curve of Type Ibc supernovae are also discussed.

Subject headings: stars: magnetic fields — supernovae: general

1. Introduction

Light curves of supernovae vary significantly. Even within the same supernova type, a spread in the shape of the light curves is found. So far, the differences have not been quantified in terms of a spread in the integrated bolometric light curves, but rather in terms of the light curves in the various broad-band filters (Hamuy et al. 1996a,b; Riess, Press & Kirshner 1996).

From the theoretical point of view, several factors can induce changes in the evolution in luminosity within a sample of supernovae of the same type: different distributions of radioactive material in velocity space resulting from differences in the burning propagation along the star, a spread in total masses of the ejecta, or a diversity in the configuration and intensity of the magnetic field, B , of the stars prior to explosion.

Very few studies have been done on the evolution of the magnetic field of a star which explodes, and how this affects its overall luminosity. In particular, little attention has been devoted to the fate of the original magnetic field configuration, which should experience a drastic change due to the enormous expansion undergone by the supernova ejecta. That can bear observable consequences in the evolution of the luminosity of the supernova.

The progenitor stars of thermonuclear supernovae are appreciably magnetized objects. Magnetic fields of WDs have been measured and range from 10^5 to as much as 5×10^8 G (Liebert 1995). Prior to the explosion, the turbulent motions inside the WD can alter the original intensity and configuration of such field by fast dynamo action. After the explosion, the huge expansion undergone by the ejecta reduces the magnetic field inside the supernova. The evolution with time of the supernova field becomes relevant to the trapping of the energy of the positrons originated in the radioactive β^+ -decays of ^{56}Co . Several hundreds

days after the explosion, if the magnetic field lines do not contribute to confine the path of the energetic positrons, with kinetic energies in the MeV range, a fraction of this energy escapes the innermost ejecta and the evolution in luminosity of the supernova is affected.

Colgate, Petschek, & Kriese (1980), and more recently Colgate (1991,1997) undertook a determination of the ejected mass in supernovae through the escape of β^+ energy in the tail of the light curves. Significant departures from the ^{56}Co -decay full-trapping curve are argued in those works. Axelrod (1980), on the other hand, suggested in his SN modeling that a chaotic weak magnetic field of $B \approx 10^{-6}$ G after the explosion would confine the positrons up to late phases. Under the later assumption, the late decline in luminosity approaches the ^{56}Co -decay full-trapping line, although positron energy is not fully deposited (Chan & Lingenfelter 1993). Whereas in earlier works a particular configuration of the magnetic field has been assumed, in the present work, we look at the processes undergone by the WD prior to explosion and as it expands, and predict how the magnetic field contents might evolve. The suggested evolution should then be compared with the observations through the predictions of the supernova luminosity.

In thermonuclear supernovae (i.e. Type Ia supernovae, or SNe Ia), depending on whether the diversity among the bolometric tails is moderate (of the order of 10–15%) or larger (≥ 30 –50 %) in the fraction of energy deposited, one would favor different mechanisms to explain this diversity. As will be shown in this work, moderate diversity suggests different distributions of radioactive material in velocity space, and a larger diversity implies differences in the magnetic field in the ejecta, and possibly also differences in the ejected mass. The information on the post-explosion magnetic field derived from the SN late

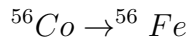
luminosity can be linked to the nature of the pre-explosion magnetic field.

In the case of Type Ibc supernovae, the effect of mixing in the deposition of energy from both γ -rays and positrons is examined as an important factor in determining the final shape of their light curves.

In Sections 2 and 3, γ -ray and β^+ -energy deposition calculations of supernovae are presented. In section 4, it is shown how in SNe Ia both mass and nucleosynthetic distribution as well as pre and post-explosion magnetic field, can be investigated through the study of the bolometric light curves. The present understanding of the evolutionary stages previous to explosion, and the duration of processes such as turbulent convection in accreting WDs, are examined in order to establish the changes of the WD magnetic field. In Section 5, the diversity of bolometric declines is presented in terms of the physical processes from which it can originate. The influence of different nucleosynthesis and kinematics of SNe Ia in the final luminosity is discussed. Mixing in supernovae of core-collapse with small ejected mass such as Type Ibc, is discussed for its effects on the bolometric luminosity within the whole core-collapse SN class as well as its incidence on the derivation of the ejected mass for those low-mass ending stars. Finally, in Section 6, we infer from the study of positron escape in supernovae some consequences for the origin of the 511 keV positron annihilation line in our Galaxy.

2. Radioactivity from ^{56}Co : γ -rays and positrons

In supernovae, the radioactive decay



provides the source of luminosity along the tail of the light curve. Such a decay has a half life of 77 days and 81% of the time gives rise to a γ -ray photon and 19% to a e^+ . γ -ray photons are emitted with a spectrum of energies reaching up to 1.4 MeV, and carry about 96.5 % of the energy of the ^{56}Co decay. The emitted positrons have an energy spectrum extending up to the endpoint kinetic energy $E_{max}=1.459$ MeV, and they account for 3.5% of the energy of the ^{56}Co decay. The fate of this 3.5 % of energy is crucial at late times.

Compton scattering of the emitted γ -rays is the main process degrading the energy of the photons as it is transferred to the electrons of the gas which become nonthermal. The comparative simplicity of the process degrading the energy of the γ -rays in expanding ejecta allows us to calculate accurately the energy deposited and the escape of energy as well.

Transport calculations of the γ -rays provide the fraction of radioactive energy deposited in the supernova ejecta as a function of inner mass fraction and time. The deposition function $D_\gamma(t)$ is a decreasing function of time as the supernova expands. The final injection of energy in the supernova ejecta takes place at a rate:

$$\begin{aligned} \xi(t) = & (6.76 \times 10^9 D_\gamma(t) + 2.72 \times 10^8 D_\beta(t)) \left(e^{-t/\tau_{Co}} - e^{-t/\tau_{Ni}} \right) \\ & + 3.91 \times 10^9 D_\gamma(t) e^{-t/\tau_{Ni}} \text{ erg g}^{-1} \text{ s}^{-1} \end{aligned} \quad (1)$$

where $\tau_{Ni}=8.8$ days and $\tau_{Co}=111.26$ days are the e-folding times for radioactive decay of Ni and Co respectively, and D_β is the deposition function of e^+ energy, whose importance becomes crucial as the ejecta become transparent to γ -rays. The term related to the decay $^{56}\text{Ni} \rightarrow ^{56}\text{Co}$ is relevant for the early rise to maximum luminosity.

Once γ -ray photons suffer Compton scattering either they do not lose a

significant amount of energy (forward scattering), or they lose significantly their energy, becoming unable to produce further energetic electrons. This has suggested the adequacy of treating the Compton scattering process as an absorption process, for applications related to the energy deposition of γ -rays (Sutherland & Wheeler 1984). A similar approach to that developed by those authors is used to calculate γ -ray transport in this work. Two methods of calculation of the deposition of energy were previously compared: the “absorption” approach generalized for an arbitrary ^{56}Ni distribution was tested against detailed Monte Carlo calculations. As found by previous authors (Swartz, Sutherland, & Harkness 1995) both results gave a very similar deposition function. Background models such as the W7 model by Nomoto, Thielemann, & Yokoi (1984) were used for these tests.

As one follows the evolution of the bolometric light curve of SNe along the ^{56}Co tail, different phases can be outlined. For SNe Ia, the post-maximum decline of the light curve is primarily determined by the temporal evolution of $D_\gamma(t)$. The luminosity at that phase and its rate of decline are related to the degree of escape and deposition from those energetic photons. That degree depends on the distribution of ^{56}Ni in the velocity-mass space, and on the total optical depth of the ejecta. This suggests defining a Δm_γ^{100} as the number of bolometric magnitudes of decline per day during the phase when γ -rays are the main contributors.

Later on, D_γ falls below the contribution of energy by positrons. At that time a new inflection in the bolometric light curve shape occurs linked to the slower evolution in time of $D_\beta(t)$. The steepness of the decline is then related to the distribution of the radioactive ^{56}Co , the velocity structure, and to the intensity and configuration of the magnetic field. As we will see, different

behaviors are expected and they can give clues to the mechanism of explosion. What happens in the phase when positrons are the dominant luminosity source depends very much on B.

When positrons in supernovae start to play a major role in the energy input (as soon as τ_γ becomes very small), the fraction of escape and deposition of the kinetic energy of those particles establishes the luminosity. The most energetic positrons and those emitted in the outer layers may succeed escaping the ejecta without becoming thermalized. A numerical evaluation is required once the supernova physical properties are known. The energy spectrum of the positrons covers a broad range of energies with a distribution of the form:

$$S(\epsilon) \propto F(Z, \epsilon)(\epsilon_0 - \epsilon)^2 \epsilon \sqrt{\epsilon^2 - 1} \quad (2)$$

where ϵ is the total positron energy in units of $m_e c^2$; $\epsilon_0 = E_{max}/m_e c^2 + 1$, E_{max} being the maximum kinetic energy; and $F(Z, \epsilon)$ is a correction for the Coulomb interaction with the final nucleus of electric charge Z (Segré 1977):

$$F(Z, \epsilon) = \frac{2\pi\xi}{1 - \exp(-2\xi)} \quad (3)$$

with

$$\xi = -\frac{Ze^2}{\hbar v} = -\frac{Z\alpha}{\sqrt{1 - \epsilon^{-2}}} \quad (4)$$

where $Z = 26$, v is the speed of the positron, and α is the fine-structure constant (Segré 1977).

Positrons with β as large as 0.94 ($\beta = v/c$) are produced in the decay. Given the initial range of kinetic energies – in the keV and MeV range –, the positrons slow down in the supernova ejecta mainly by ionization and excitation losses. At higher energies, bremsstrahlung would be the dominant energy loss mechanism,

and at lower energies, Coulomb scattering would be dominant (see Segré 1977, for instance).

As the positrons slow down due to their loss of energy in the ejecta, they travel a fraction of the envelope which can be estimated as the *stopping distance*, d_e due to ionizations and excitations in the SN Ia envelope.

The full relativistic expression for positron energy loss, per unit length, X , due to ionization of atoms is (Heitler 1954; Blumenthal & Gould 1970; Gould 1972):

$$\frac{dE}{dX} = -\Gamma(E) = -\frac{4\pi r_0^2 m_e c^2 Z \rho}{\beta^2 A m_n} \ln \left(\frac{\sqrt{\gamma - 1} \gamma \beta}{I/m_e c^2} \right) + \frac{1}{2} \ln 2 + \Sigma_2(E) \quad (5)$$

where E is the kinetic energy, r_0 is the classical electron radius, m_n is the atomic mass unit, Z and A are, respectively, the effective nuclear charge and atomic mass of the ejecta material, and $\Sigma_2(E)$ gives the relativistic factors as a function of the Lorentz factor, γ , and of β (Berger & Seltzer 1954).

I is the effective ionization potential for the ambient atoms in the ejecta. A semiempirical formula for the ionization potential gives (Roy & Reed 1968; Segré 1977):

$$I = 9.1Z \left(1 + \frac{1.9}{Z^{2/3}} \right) eV \quad (6)$$

Due to the weak dependence of dE/dX on I , the formula above for I is accurate enough for the practical calculation of the energy loss.

The *stopping distance of the positron* as result of impact ionization and excitation in a SN Ia envelope is found to be approximately:

$$d_e \equiv \frac{E}{-dE/dX} \approx \frac{3.36}{\rho} \left(\frac{E}{m_e c^2} \right) \frac{A}{Z} \left(\ln \frac{E}{I} \right)^{-1} cm \quad (7)$$

In Table 1 some typical values are given for d_e , the *stopping distance of the positrons* of different energies both for Chandrasekhar WDs and WDs of the smallest possible exploding mass. Synchrotron losses by the e^+ in the presence of the magnetic field, bremsstrahlung losses, and losses due to Compton scattering off photons contribute to the slowing down of the positrons to a much lesser extent.

Each magnetic field configuration specifies in a given way the positron transport in the supernova ejecta. We have specified three likely configurations of the field lines, and adopted an efficient way to calculate the deposition function. Three situations which the positrons might encounter in exploded ejecta are: a *chaotic magnetic field background* (a likely result of the turbulent motions prior to explosion), a *radial field* (resulting from expansion of the original dipole field in fast moving ejecta), or *the absence of a significant magnetic field*, in which case they are just subjected to their interactions with ions and electrons along free trajectories.

The deposition calculation consists in determining how efficiently the relativistic positrons transfer their energy to ions and electrons increasing the kinetic energy of the latter: positrons thermalize if they release most of their kinetic energy. That energy should reappear as optical–infrared luminosity through the excitation of a whole range of transitions or through ionization and recombination processes. In the present work, the confinement of positrons in a chaotic magnetic field is first investigated. Positrons of different energies are followed through their interactions over time, testing whether they become thermal or whether they remain nonthermal within the ever more diluted ejecta. The positron mean free path is very small as compared with the characteristic radius of the supernova ejecta when the density of the ejecta is still high enough

to produce large losses of the positron energy by ionization and excitation, or when the presence of a turbulent magnetic field inside the ejecta confines the trajectories of the positrons along the winding field lines and induces a larger number of interactions. The mean free path of the positron becomes large when either the density of the ejecta is too low to slow down the positrons or the energy density of the magnetic field is extremely low and therefore the Larmor gyroradius of the particle is a sizeable fraction of the radius of the ejecta. In the latter case the escape is enhanced. The distance travelled by the positron increases when a strong radial magnetic field confines the positrons to move out in their helical motions along the radial field lines.

In the presence of a background chaotic magnetic field, positrons of energy E_i born at a given radius r_i (of mass coordinate m_i and velocity v_i) cannot slow down to thermal energies if they are emitted after a critical time $t_i > t_c(m_i, E_i)$. The turbulent magnetic field confines the positrons at their site of origin, but as the ejecta expand and decrease in density, the possibilities for thermalization decrease. Thus, a fraction of the energetic positrons will not successfully thermalize even under confinement and survive in the ejecta as a “fast”, nonthermal population. The critical time for thermalization depends on the gradient of velocity along the ejecta, on the energy of the positrons, and on their rate of energy loss. A useful expression to evaluate such critical time is given by Chan & Lingenfelter (1993):

$$t_c(m_i, \gamma_i) = \left[\frac{8\pi m_e c v_{sn}^2(m_i)}{M} \left(\frac{dv_{sn}}{dm} \right)_{m_i} \times \int_1^{\gamma_i} \frac{\gamma}{\Gamma(\gamma m_e c^2) \sqrt{\gamma^2 - 1}} d\gamma \right]^{-1/2} \quad (8)$$

where M is the mass of the ejecta, $v_{sn}(m_i)$ is the velocity of the supernova ejecta at m_i , $(dv_{sn}/dm)_{m_i}$ is the velocity gradient at the location of m_i , and $\Gamma(E)$ is the energy loss due to the different processes. Chan & Lingenfelter (1993) included

among those processes impact ionization and excitation, whereas we found that one should include as well Coulomb scattering (Bhabha scattering involving e^+e^- , in this case), since this is also a major process in the deposition of energy of positrons. Our algorithm differs from that from those authors in the inclusion of this additional process as degrading the positron kinetic energy, and also in the focus of the calculations: the main quantity for light curve calculations is the energy deposited in the supernova, instead of the energy escaping as energetic positrons.

In the second configuration considered here, the confinement of positrons in a chaotic magnetic field is substituted for a different frame: the particles travel along the lines of a radial magnetic field. Again, $\Gamma(E)$, the energy loss function, and the mass of the ejecta will determine the fraction of kinetic energy that they deposit. The equation for the trajectory has to be solved simultaneously with the energy loss equation.

$$r = v_{sn}(m_i) t_i + \int_{t_i}^t c\beta(t')\cos[\theta(m, t')]dt' \quad (9)$$

given an initial mass coordinate m_i and pitch angle θ_i . The changes in pitch angles due to the gradient in $B(r,t)$ outwards, favor a forward beaming of the positrons in the radial direction, even if they were emitted with θ_i close to $\pi/2$ (Colgate, Petschek, & Kriese 1980; Chan & Lingenfelter 1993).

A last option is the absence of any significant magnetic field able to affect the trajectory of the particle. In that case, positrons are not confined to follow any trajectories and a treatment similar to γ -ray transport can be used, adopting the appropriate absorption coefficient for the positron processes.

The default values given in the Tables for bolometric magnitude declines correspond to the chaotic field case, but decline rates in the absence of magnetic

field and in the case of a radial field will also be mentioned when comparing models with observations.

3. Time evolution of the bolometric magnitude

3.1. C+O WD ignition and structure of the radioactive source

The degree to which differences observed in the evolution in luminosity of supernovae are linked to the distribution of radioactive sources and the kinematic structure of the exploded star has hardly been quantified. The central ignition of a C+O WD with a mass close to the Chandrasekhar mass produces a ^{56}Ni distribution buried from the center up to variable mass fractions, depending on the characteristics of the burning front. In the alternative edge-lit detonations of C+O WDs, burning starts at the outermost layers of the star and proceeds towards the center. In those explosions, the radioactive material is found at two different locations: very near to the surface, where the ignition started, and around the center where, after propagation of the burning front, the densities of the interior favor burning to NSE (Nuclear Statistic Equilibrium) products.

Within both frames for the explosion of a SNIa, variations in the total mass of ^{56}Ni and of its location in velocity space are found, related to the extent to which the burning front incinerates the material. Classical Chandrasekhar central ignition models are able to incinerate $0.6 M_{\odot}$ of the star to ^{56}Ni . The nucleosynthesis and density structure of the class is well represented by model W7 (Nomoto, Thielemann, & Yokoi 1984), where $0.63 M_{\odot}$ of ^{56}Ni are buried below the surface of 9000 km s^{-1} . This model is known to provide a good spectrum for “normal SNe Ia”. In the case of Chandrasekhar explosions, very ^{56}Ni -poor explosions can also be found when the WD undergoes a pulsation that changes the mode of propagation of the burning front (Khokhlov 1991). The

pulsating delayed detonations can produce a low amount of ^{56}Ni in the center, which is buried at low velocities and very low mass fractions. An example of such model is the here depicted model WPD1 (Woosley 1997), suggested to account for subluminous SNe Ia.

Among sub-Chandrasekhar models, a range of possible explosions corresponds to the ignition of WDs of different masses (Woosley & Weaver 1994; Livne & Arnett 1995). Results from 1-D and 2-D hydrodynamic calculations give similar final structures for the ejecta, and a whole range of possible structures corresponding to the ignition of WDs of different masses. An exploded WD of mass $\simeq 0.97 M_{\odot}$ synthesizes the same amount of ^{56}Ni as W7, but it contains this radioactive element also in the outermost layers (model 6 by Livne & Arnett 1995, for instance). The detonation of a $0.7 M_{\odot}$ C+O WD synthesizing about $0.15 M_{\odot}$ of ^{56}Ni corresponds to the lowest end of possible WD masses able to explode by edge-lit detonations (model 2 by Livne & Arnett 1995 represents such a structure). It is a candidate to explain very subluminous SNe Ia. On the highest end in luminosity, the detonation of a $1 M_{\odot}$ C+O WD provides the largest amount of ^{56}Ni ($\simeq 0.97 M_{\odot}$). As representative of the top end, we investigate a model by Nomoto (1994). Table 2 summarizes the characteristics of the models investigated here as possible structures of exploded WDs.

3.2. $D_{\gamma}(\mathbf{r})$ and Δm_{γ}^{100} in Type Ia supernovae

The bolometric light curve in the phase where the γ -rays fuel the luminosity is well described by the decrease between one hundred and two hundred days after the explosion. We can define M_{bol}^{100} as the bolometric magnitude at 100 days after explosion and Δm_{γ}^{100} as the number of bolometric magnitudes declined

per day after 100 days. During the period where Δm_γ^{100} measures the decline rate due to the increasing transparency of the envelope to γ -rays, the SNIa models of lower mass do not experience a larger change of magnitude than the more massive ejecta. This is due to the fact that the γ -rays of the outermost ^{56}Ni have always escaped easily, and, on energy deposition effects they were not important. The inner structure of the deposition function shows a peak at the innermost radii as in the Chandrasekhar models, and the density structure is somewhat flatter in less massive WDs. The luminosity of Chandrasekhar models is, however, higher than that of low-mass models because the total ^{56}Ni mass being equal, the effectively buried ^{56}Ni relevant for γ -ray trapping is larger than in the edge-lit cases, and the optical depth is larger (more mass). Table 3 gives the values for Δm_γ^{100} , and absolute magnitudes for various models.

Figure 1 shows by the example of subluminescent SNe Ia resulting from the sub-Chandrasekhar explosion of a $0.7 M_\odot$ (model 2 by Livne & Arnett 1995) or from a pulsating delayed detonation (model WPD1 by Woosley 1997), the level of deposition of γ -rays of the supernova at late phases. The model of pulsating delayed detonation achieves a higher luminosity than the sub-Chandrasekhar edge-lit detonation of a $0.7 M_\odot$ WD. The Figure also shows how most of the emission comes from the inner 20% fraction of mass.

If ^{56}Co would only give γ -rays, we would never see the 50–80 % of mass fraction in SNe Ia at late phases. Since the γ -ray-sphere (if we define it as the sphere which concentrates more than 80% of the deposition in energy) has shrunk down to the 20% inner mass fraction or even deeper, we would only see emission at very low velocities. Due to the role of positrons and to their flatter deposition function, this does not actually happen. Positrons stop the drop in luminosity of the supernova ejecta.

3.3. Decline in the positron tail

Leaving aside the discussion on the magnetic field intensity (it will be addressed in the next section), it is clear that some inner structures of exploded WDs are more favorable to trapping of positrons than others. The effect can start to become evident as early as 200 days after the explosion. For larger velocity gradients, and ^{56}Ni placed outside the inner regions, the escape of positron energy is enhanced. The escape strongly depends on the velocity gradient along the ejecta and on the distribution of the radioactive source. Better trapping structures are centrally-ignited Chandrasekhar C+O WDs, as compared with edge-lit C+O WDs. If we determine the *number of magnitudes declined per day in the bolometric light curve between 200 and 400 days*, $\Delta m_{1\beta}$, and *between 400 days and 1000 days*, $\Delta m_{2\beta}$, a good clue as to the right model can be achieved. The expected values for some representative models are given in Table 3. Table 3 compares the rate of decline between 200 and 400 days when positrons are the main energy source with that later on, between 400 and 1000 days, when they might fail to fully deposit their energy, depending on the post-explosion structure of the supernova. This Table stresses the intrinsic differences due to the kinematics and distribution of radioactive material in different models. The calculations have been done assuming confinement by B within the ejecta. In Section 5 we relax this requirement in view of the existing observations.

The difference in deposition of positron energy at 300 days and 350 days for the abovementioned SNe Ia models, if the magnetic field succeeds in providing enough trapping in the ejecta, is displayed in Table 4. As it can be seen, escape in sub-Chandrasekhar WDs can reach up to 20% after 200 days. In Figure 2 the deposition function of the β^+ energy shows different behaviors for the different

models from 200 to 1000 days. In a Chandrasekhar model like W7 even with a turbulent configuration of the magnetic field, at 740 days after the explosion the positrons do not deposit their energy totally. However, the departure is only moderate (10%). If the configuration of the magnetic field were radial, or the magnetic field intensity were very low, significant departures from full trapping could be achieved even earlier.

4. Magnetic field of the WD: pre and post-explosion

Either full confinement of positrons in a chaotic magnetic field (Axelrod 1980), or an enhanced escape through a radially combed out configuration (Colgate, Petschek, & Kriese 1980; Colgate 1991) have been considered as limiting cases for the magnetic field in the SN ejecta. From current knowledge of the pre-explosion structure of the WD, and following the effects of expansion, we can reexamine these issues.

Some WDs are known to host magnetic fields of intensity ranging between 10^5 and 10^9 G (Liebert 1995). Such high magnetic fields are not common, however. Most WDs probably have fields below the detection limit of 10^4 – 10^5 G. A number of studies suggest that the configuration of the magnetic field is generally more complex than a dipole (non-centered dipolar geometry or quadripolar), and that the strength of the magnetic field might be correlated with the mass of the WD in the sense of more massive WDs hosting larger magnetic fields. This last point, however, has not been established on a firm statistical basis.

Prior to the huge expansion induced by the explosion, however, the mass-accreting WD progenitor of the SNe Ia goes through a stage which might increase the intensity of its initial magnetic field. Thermonuclear runaway, which

initiates the explosion, is preceded by a stage of quasistatic C burning that creates a central convective core (Woosley et al. 1990; Niemeyer & Hillebrandt 1995). As already found by Arnett (1969), when C burning accelerates after C ignition, electron conduction alone becomes unable to transport the ever larger energy flux and the temperature gradient becomes superadiabatic. Therefore, turbulent motions develop, encompassing a sizeable fraction of the WD interior. The interaction of the turbulence with the magnetic field should thus be examined, in order to see whether an initially small B might be significantly amplified during the steps immediately preceding the explosion.

A magnetic field wound up by turbulence increases with time, until the field strength becomes strong enough to resist the turbulent flow. Since we are interested in weak fields, we may ignore here such backreaction by the Lorentz forces. The precise rate of increase of the field depends on the details of the small-scale flow. For a flow dominated by a single length scale Kraichnan (1976) has derived exponential growth on a time scale of the order of the turnover time τ of the flow. Thus, wrapping up of field lines by a small scale flow can enhance the intensity of the magnetic field exponentially:

$$B_{\text{seed}} e^{t/\tau} \text{ where } \tau \approx l/v_{\text{turb}} \quad (10)$$

τ being the typical turnover time of the convective cells, which is of the order of the ratio of characteristic length of the turbulent region over the turbulent velocity. If the duration of a turbulent period allows for a few turnovers of the turbulent material (t larger than τ), the lines of the magnetic field would be wrapped a few times, and the intensity would increase. This effect is not the classical dynamo where the field is amplified as cyclonic motions twist the lines of the magnetic field in a rotating fluid. The action examined here is linked to

the turbulence-induced winding up of the lines as the eddies carrying the seed magnetic field undergo several turnovers.

Therefore, prior to explosion, during the quasistatic burning of C, an enhancement of B can occur. The result depends on the duration of the turbulent quasistatic phase.

If the turbulence lasts for more than a few turnovers, equipartition of the kinetic energy density and magnetic field density could be achieved. In equipartition:

$$\frac{1}{2}\rho v^2 = \frac{B^2}{8\pi} \quad (11)$$

Taking characteristic values for the turbulent kinetic energy density, i.e 10^{11} erg g^{-1} and given that ρ is $\approx 2-3 \cdot 10^9$ g cm^{-3} , B values for equipartition are $\approx 10^{10-11}$ G.

The convective phase prior to explosion is found in the work by Woosley (1990) to last for $\approx 10^{2-3}$ s. Turbulent velocities are of the order of a 10^{5-6} cm s^{-1} and the convective core is a fraction of the WD radius of typical $l \leq 10^7$ cm. This implies turnover times of $\tau \approx 100$ s. In the work by Arnett (1996) and Bravo et al. (1996), the pre-explosion evolution of the WD during the accretion process is followed in detail several thousand years prior to explosion. Both works find independently that a convective core develops several thousand years prior to the explosion. Turnover timescales are of the order of 300s. The convective period is of the order of 10^{10} s, long enough, according to (10), to rise the magnetic field strength to equipartition values. Such a convective core is linked to the evolution towards explosion of centrally ignited Chandrasekhar C+O WDs. In edge-lit detonations of sub-Chandrasekhar WDs, there is no such development of convection in the C+O core in the presupernova evolution

according to the calculations by Nomoto (1982) and Hernanz et al. (1997), since in this kind of explosion there is no strongly peaked central heating of the WD before the shock wave generated at the surface reaches the center and induces the explosion. Therefore, the initial field configuration in the core of the WD would not have been significantly distorted. The post-explosion configuration for the two types of explosion would then be different and its effect on the light curves can help to determine the SNIa mechanism.

Thus, depending on the evolution towards explosion, the dynamo might have had enough time to efficiently increase the intensity of magnetic field by large factors, or fail to do so. The effects of a failure to increase drastically the mean intensity of the field will be reflected by the supernova light curve.

If this phase fails to develop an entangled field, the following phases do not favor any major change.

When the incineration starts, the turbulent velocities increase to 10^7 cm s^{-1} , and the characteristic size of the turbulent region is of the order of 10^7 cm (Niemeyer & Hillebrandt 1997). However, this phase lasts only ≈ 1 sec, and it would not be able to provide a sufficient enhancement of the magnetic field in the ejecta.

After the explosion of the WD, the ejecta undergo a large expansion. The homologous expansion achieved about 1 sec after the explosion suggests the further conservation of the magnetic flux (there is no compression which would distort the number of lines crossing a given element of area). In a homologous expansion all components of the field decrease like:

$$\frac{B_1}{B_0} = \frac{(R_0)^2}{(R_1)^2} = \frac{(R_0)^2}{(v \times t)^2} \quad (12)$$

Though the overall flow is nearly homologous on a large scale, there is likely

to be some form of small scale motion inside the ejecta. For example, this could be a remnant of the convective motions in the pre-SN stage, or the result of a Rayleigh–Taylor instability at an early stage during the explosion. Such motions wind up field lines, causing again a roughly exponential growth of the field strength, in the kinematic (low field strength) limit. The question thus arises if such a process could increase the field strength over that expected from a purely homologous expansion. We can now show that this is not the case except in the unlikely event that the overturn time of the small scale motions is less than the expansion time scale.

Small scale motions generated at any time t_0 during the expansion expand with the flow, so that their length scale varies as t/t_0 . The flow velocity in these motions will remain the same or decrease in the presence of dissipation, hence the turnover time scales at least as t/t_0 . Hence in the absence of overall expansion, we would expect the field to increase as $d \ln B/dt \approx 1/\tau$. Due to the expansion the overturning time varies as $\tau = \tau_0 t/t_0$, where τ_0 is the initial overturning time and $t_0 = R_0/v$ the initial expansion time scale. Thus, because the overturning time increases with time, the growth of the field is no longer exponential. The expansion (using eq 12) changes the field at a rate $d \ln B/dt \approx -2/t$. Adding these contributions, we get

$$\frac{d \ln B}{dt} = \frac{1}{\tau} - \frac{2}{t} = \frac{1}{t} \left(\frac{t_0}{\tau_0} - 2 \right) \quad (13)$$

This shows that the decrease of the magnetic field by expansion dominates as long as the initial turnover time of the small scale motions is sufficiently long compared with the initial expansion time scale. For an initial expansion time scale of less than a second, this condition is easily satisfied by any small scale motions in the pre-SN. We conclude that the first term on the right in (13) can

be ignored, and that the magnetic field decreases according to eq (12), even in the presence of small scale motions in the expansion.

Whatever magnetic field was present before the onset, at the quasistatic burning phase of C, will be directly left to the effects of the overall expansion of the ejecta, which tends to lower its intensity.

After the explosion, the flux of the magnetic field would be preserved, and should be decreasing with t^{-2} as the supernova expands. *At 100 days the intensity of the magnetic field would have decreased by a factor of 10^{-15} .* At 1000 days it would be decreased by 10^{-17} . The ejecta can thus host magnetic fields much lower than the intensity of the interstellar magnetic field, if the magnetic field in the WD has not been significantly enhanced prior to explosion. Taking, for instance, an initial magnetic field of 10^4 G, at 100 days it will be as weak as 10^{-11} G, and at 1000 days it will be 10^{-13} G. The magnetic energy density will be among the lowest ones in known astrophysical objects. The supernova becomes a huge de-magnetized bubble (with a material density much higher than the surrounding medium, though).

The low values of B should, however, be compared with the dimensions which the ejecta have achieved.

For a charged particle of charge q , moving in a magnetic field, B, with velocity v whose component perpendicular to the direction of the magnetic field is v_{trans} , the gyroradius (or Larmor radius) is:

$$r_{gy} = \frac{mc\gamma v_{trans}}{qB} \tag{14}$$

where m is the mass of the particle and $\gamma = [1 - (v^2/c^2)]^{-1/2}$.

For a positron of energy 1 MeV, the gyroradius would be:

$$r_{gy} = \frac{4.7 \times 10^3}{B} \quad (15)$$

Thus, the gyroradii of the e^+ , as compared with the size of the envelope would be:

$$x_\xi = \frac{r_{gy}}{R} = 4.7 \times 10^3 \text{cm} B_0^{-1} R_0^{-2} (v t) \quad (16)$$

This is of the order of:

$$x_\xi = 10^{-5} t_7 B_{08}^{-1} \quad (17)$$

where B_{08} is the magnetic field before expansion in units of 10^8 G and t_7 , the elapsed time since the explosion in 10^7 s. Depending on the B_0 value, the positrons can be more or less trapped inside the ejecta. Less energetic particles have smaller gyroradius. When the magnetic field has diluted down to very low values, the gyroradius encompasses a high fraction of the expanded ejecta.

A pre-expansion magnetic field of 10^{11} G would prevent large departures from full-trapping of ^{56}Co at phases even later than 1000 days after explosion. The confinement requirements are seen from equation (17). The available observations on the late bolometric decline of the light curve allow us to estimate if a departure from the full-trapping decay line occurs in SN. *This leads to an estimate of the intensity of the magnetic field achieved before the homologous expansion.*

4.1. Possible magnetic shield around the supernova ejecta

The field strength in the ejecta may become sufficiently low after 100–1000d to allow the positrons to travel through the ejecta without interacting with the field. If the magnetic field of the WD is a dipole magnetic field, and the

ISM around the ejecta is dense enough to present significant opposition to the magnetic field expansion, the conditions on final escape of positrons might change.

Before the particles can be regarded as having successfully escaped from the ejecta, it must be shown that they are not reflected back into the ejecta by an external medium of sufficient density. This external medium consists of two regions. Immediately outside the ejecta is a magnetic ‘shell’, a region dominated by the external magnetic field of the original pre-SN core, now expanded but still containing the original amount of magnetic flux. Outside this shell is the ISM, modified by the SN shock that has passed through it. The magnetic pressure in the shell has to balance the ram pressure of the ISM relative to the ejecta. This yields its field strength:

$$B_s = v(4\pi\rho_I)^{1/2} = 0.04n_I^{1/2}v_9\text{G} \quad (18)$$

where v_9 is defined such that $v = 10^9v_9$ is the velocity of the ejecta and n_I the ISM particle density. The flux of field lines crossing the magnetic equator is conserved during the expansion, and is of the order $2\pi B_0R_0^2$, where R_0 and B_0 are the radius and surface field strength of the WD. At time t , the thickness d of the shell is therefore:

$$d = R_0^2B_0/(vtB_s) = 2 \cdot 10^7 \frac{B_{04}R_9^2}{n_I^{1/2}v_9^2t_7} \text{ cm} \quad (19)$$

where B_{04} is the magnetic field in units of 10^4 Gauss, R_9 is the radius of the WD in 10^9 cm. The gyroradius of a 1MeV positron in this field is:

$$\frac{r_L}{d} = 5 \cdot 10^{-3} B_{04}^{-1} v_9 t_7 / R_9^2 \quad (20)$$

Since the field is parallel to the interface with the ejecta, the shell presents an effective ‘shield’ which reflects the positrons.

Thus we may reasonable assume the shell around the ejecta to be a near perfect reflector. If the positrons inside it are unconfined due to the absence of a tangled field, they will spread uniformly through the ejecta. The mass of the ejecta is concentrated towards the innermost radii. If the half-mass radius is at a fraction $f \sim 0.1 - 0.2$ of the radius of the envelope, the central density of the uniformly spread positrons is of the order $\sim 2f^3$ times what it would be if the positrons stayed trapped near their source in the high-density regions. Since the luminosity is proportional to the density of positrons in the region containing most of the mass, the reduction of the luminosity is likely to be a large factor, even if none of the positrons actually escape from the ejecta.

5. Bolometric declines and their interpretation

5.1. Physical conditions in the SN envelope and their effects on the departures in the bolometric light curve

Both a weak magnetic field and the progressive thinning out of the ejecta produce a departure in the bolometric light curve of supernovae from the full-trapping of the ^{56}Co -decay energy. There is no possibility of having 100 % trapping of positron energy as time goes by. The case where this departure occurs at the earliest, is when there is no confinement of positrons at their site of origin, as discussed before. If the positrons are freely streaming or escaping through a radial magnetic field, the time required by the relativistic e^+ to cross the ejecta is shorter than any relevant timescale for modifications in the physical conditions of the envelope, such as the the radioactive timescale for ^{56}Co -decay (111.26 days) or the expansion timescale ($n/\dot{n} = t/3$ days), both being of the order of 100 days. In the free-streaming condition, the moment

when the departure occurs is early enough to ensure that any deposited energy is radiated in a short timescale through collisional excitation and emission in a large number of forbidden transitions of iron ions. Freeze-out conditions for re-radiation of that energy occur much later.

In the confinement phase, the positrons do not move from their site of origin. There is a time when the probability of interaction with the ions through impact ionization and excitation becomes very low. Although the follow-up of the deposition of energy by the energetic particles involves to keep track of the old positrons during the whole expansion history of the envelope while injecting the new ones at each site, the fact of neglecting them when they start to become very inefficient, i.e after $t > t_c$ (see section 2), is a fair approximation. The probability for interactions decreases with t^{-3} and the contribution of all those positrons in the diluted medium is much smaller than before, at $t > t_c$. At the latest times, the quantitative prediction can underestimate somehow the luminosity. The estimate of the time at which the departure occurs according to the physical SN model and magnetic field configuration, is, however, very precise.

Timescales and expected departures

The frequency of impact ionizations or excitations by the e^+ becomes lower as n_{e^+} , the density of the energetic positrons, and that of the target ions decrease. The timescale for impact ionizations by positrons, τ_{e^+coll} , can be expressed as:

$$\tau_{e^+coll} = \left[\int_{E_{min}}^{E_{max}} n_{e^+}(\tilde{E}) \int_0^{\tilde{E}} \sum_{ij} \sigma_{ij}(E) v_E f_{ij} dE \right]^{-1} \quad (21)$$

where $n_{e^+}(\tilde{E})$ is the number density of positrons of a given energy \tilde{E} originated in the ^{56}Co decay, σ_{ij} are the impact ionization cross sections with each target

ion i of species j and f_{ij} are the relative abundances of those ions. E_{\min} and E_{\max} are the minimum and maximum kinetic energy of the positrons, and v_E the velocity. $n_{e^+}(\tilde{E})$ is much lower than n_e , the electron density. Such timescale increases due to the thinning out of the ejecta, and at a given point it becomes larger than the radioactive timescale and the expansion timescale.

Equivalently, the timescale for the positrons to lose half of their energy, τ_{e^+loss} , becomes also large (this quantity is related to the stopping distance of the positron, which grows with time, see Table 1):

$$\tau_{e^+loss} \sim \frac{E}{\bar{E}} \quad (22)$$

In *the confinement regime*, the rate at which interactions occur is favored by the presence of a uniform density of target ions along the positron path. The departure occurs much later than in *the free-streaming regime* for all models. This departure signals a point of “breakout of nonthermal ionization balance” or “non-steady state for the nonthermal processes”. However, the collisional processes and radiative transitions between levels still occur at a fast rate. Reemission is occurring through the large number of forbidden transitions of iron ions. The deposited energy is reemitted, to a very high degree, in steady state.

In *the positrons free streaming regime*, τ_{e^+loss} for the most energetic positrons is longer than the crossing time of the envelope. Those positrons, which are not confined, will escape with high kinetic energies. The free streaming favors much earlier departures from full-trapping of the ^{56}Co , at epochs when the recombination and collisional processes still occur at high rates.

The infrared catastrophe: freeze-out of the supernova ejecta

The observational requirements to extract information from the bolometric

light curve of a supernova for the prospects given in this work are to rigorously reconstruct this light curve placing estimates on the infrared emission, and to complement this task with a spectrum at the time where a change in the decline rate is observed. Here, we present our predictions to be compared with future observational data. By obtaining those data, it should be possible to distinguish observationally between the various effects entering in the bolometric light curve decline.

Along this work, when addressing the departure in the luminosity, we assume that the emission at ultraviolet, optical and infrared broad bands is recovered, and an estimate of the temperature or evaluation of how much luminosity has gone into far infrared wavelengths has been done.

Axelrod (1980) first pointed out that the supernova ejecta in their late-time evolution would reach a point when temperatures would fall below a critical temperature, $T_c \simeq 2000$ K, in their innermost layers. When this occurs, most of the emission of the supernova, would come out in the fine structure forbidden transitions at infrared wavelengths. This is named as the Infrared Catastrophe (IRC) since it will imply an inflation of the emission at very long wavelengths while a depletion in the optical and ultraviolet emission occurs. It is possible to calculate for each model when T_{core} (in the innermost dense ejecta) falls below T_c , and determine it as well observationally.

The departure, when an IRC occurs, affects the B, V, R monochromatic light curves, but it is a temperature effect and does not imply a proper departure of the overall emissivity.

Limitations in the accuracy of the results of the following sections arise from the uncertainties in the observations and reconstructions of those bolometric

light curves (if a limited number of photometric data are available) and from the growing time-dependence of the reemission processes well after two years. The different predictions related to the two evolutionary histories of centrally ignited Chandrasekhar WDs and edge-lit low mass C+O WDs seem worth testing. Combining the analysis of the γ -ray tail and the positron tail helps to complement information on the physical models. This information will be addressed in the next sections.

5.2. Physical models and the rate of the late decline of SNe Ia

As a general trend, C+O centrally ignited Chandrasekhar WDs tend to trap significantly the positrons and give a bolometric light curve decline close to the full trapping line drawn by the exponential decay of ^{56}Co . The bolometric light curves of sub-Chandrasekhar models tend to fall below the full-trapping line after 400 days even if B confines the e^+ , or even earlier in massive edge-lit detonations (model NIDD by Nomoto 1995). A follow-up of those bolometric light curves is a good tool to clarify the nature of the explosion. The bolometric light curve in the earlier γ -ray dominated tail (before 200–300 days) is different for those models and allows a first discrimination. The positron tail informs further about the ejected mass and the magnetic field configuration. In Figure 4 we present M_{bol} decline rates for different models during the first 400 days under the confinement hypothesis. This sort of figure can be useful for comparison with observations. Departures from the full-trapping of ^{56}Co -decay of the order of 10–15% at about 400 days can be explained by the distribution of radioactive material. Larger departures, of 30–40 % or larger, have to be interpreted in terms of lack of magnetic field confinement of the positrons, or even enhancement of the escape.

5.3. Trapping and departure: the magnetic field and the mass of the ejecta

A way to evaluate from its physical effects the real effectivity of positron trapping is to compare the calculations with observed bolometric light curves of SNe Ia. Very few bolometric light curves of supernovae are, however, available. For SN 1972E in NGC 5253, about two years of bolometric follow-up after the explosion is provided by Kirshner & Oke (1975). Since this exceptional long-lasting coverage, the general trend has been to concentrate the observations of supernovae to the first year after the explosion. Suntzeff (1996) obtained the bolometric light curve of SN 1992A up to 300 days after explosion. More recently, the fast declining bolometric light curve of SN 1991bg covering the first two hundred days after explosion was presented by Turatto et al. (1995).

What can we learn from the observations? SN 1972E might represent a SN Ia close to “normality” in its luminosity and spectral characteristics (i.e. similar to SN 1981B, SN 1990N). The spectral scans obtained by Kirshner & Oke (1975) and integrated along wavelength by Axelrod (1980) provide a bolometric (or quasi-bolometric) light curve which can usefully be compared with model calculations. The distance to the supernova is known from the Cepheids period–luminosity relationship (Sandage et al. 1994), and it is known that the supernova was not substantially reddened ($E(B - V) \approx 0.05$). We scale the absolute luminosity values according to the known distance to NGC 5253 and a low $E(B - V)$ (Axelrod had assumed $E(B - V) = 0.22$), and compare them with the model predictions. Figure 3 shows that the SN 1972E bolometric light curve follows well the behavior of centrally ignited C+O Chandrasekhar WD with a turbulent magnetic field configuration. In particular, model W7 seems to be giving a very good account of the bolometric light curve. The turbulent

configuration of the magnetic field is thus favored by the level of deposition of energy suggested by the bolometric curve of SN 1972E prior to 500 days. A lack of magnetic field as well as a radial strong magnetic field would produce larger departures from the full-trapping ^{56}Co -decay line.

The model light curve follows well the observed one until at least 500 days. Then, a departure at 720 days after maximum is observed, of the order of 70 % enhancement of escape as compared with the confinement prediction (only 30 % of ^{56}Co positron kinetic energy is deposited). The confinement prediction gives only 10 % of departure at 740 days for model W7. Taken at face value, this reported departure, and the elapsed time in the confinement regime (in the case of SN 1972E up to 500 days according to our analysis), tell us about the magnetic field intensity prior to explosion, as discussed above. According to equation (17), the confinement of positrons starts to fail at about 700 days for WD magnetic fields of $B \approx 10^5 G$, a plausible value. If the magnetic field intensity of the initial WD would have been lower, the departure would have occurred earlier. A very magnetized WD prior to explosion ($B \geq 10^{10-11} \text{ G}$) would not give any significant departure until much later on. Unfortunately, it can not be discarded that the very last point in the light curve is more unaccurate than the rest of the data (Kirshner 1997), and that the bolometric light curve keeps falling not far from full-trapping. If that were the case, and the bolometric light curve would follow within a 10% of departure the full-trapping curve, that would confirm the theoretical expectations of a chaotic magnetic field enlarged up to equipartition during the long convective accreting period expected in centrally ignited C+O WDs. The safest conclusion given here is that *SN 1972E represents the case of a centrally ignited C+O WD with a likely tangled magnetic field of at least $10^5 G$ prior to the expansion.* The light curve

and luminosity is well reproduced by model W7.

Future observations, describing the bolometric light curves of SNe Ia, should provide information about the post-explosion magnetic field. Strong dust obscuration can cause deviation in the bolometric declines, but it is accompanied by shifts in the centroids of the emission lines at late phases. Thus, there is a way to point out when dust obscuration occurs. The light curve can be corrected by observing the far infrared and including the energy emitted at those wavelengths. The bolometric light curve of SN 1992A seems to follow the same decline rate as SN 1972E, although data are only available up to 300 days. Given the uncertainties in the distance to this supernova, we have shifted arbitrarily in the figures the absolute scale of the luminosity given by Suntzeff (1996).

5.4. A fast decaying bolometric light curve

A much faster decline than in SN 1972E is seen in SN 1991bg. Observations were presented in terms of the *uvair* bolometric light curve by Turatto et al.(1995). They followed the same procedure to integrate the luminosity in the different bands as Suntzeff (1996) for SN 1992A. Light from the far-infrared is not included in their luminosity count. However, *JHK* observations by Porter et al. (1992) showed a fast decline of 3 mag in the first month and no secondary maximum. This suggested that the supernova was not emitting strongly in the infrared.

Calculated bolometric light curves are displayed in Figure 5 and compared with SN 1991bg. The decline after 200 days (and even earlier) is faster than predicted for confinement by a chaotic magnetic field in a wide variety of models. The early decline shows that the two opposite models proposed to explain

this supernova: an edge-lit detonation (Livne & Arnett 1995) and a pulsating delayed detonation model in a Chandrasekhar-mass WD (Woosley 1997) fail to give the right luminosity and evolution in time of the bolometric light curve in the γ -ray dominated phase already. Shifting the absolute magnitude of both models to agree with the observed one would imply as well uncomfortable distances to the core of the Virgo Cluster (well beyond the current discussions on it). The bolometric light curve of SN 1991bg requires a small mass of ^{56}Ni , of the order of $0.07 M_{\odot}$, as found by spectral modeling (Ruiz-Lapuente et al. 1993). In addition to requiring a small mass of ^{56}Ni , further considerations are needed to explain the unusual late behavior. At day 200 there is a departure from the confinement prediction: the deposition is only 50% of what would be expected in the confinement case. In this case the observational basis for such departure is firmly established. Different options have to be considered: 1) a low magnetic field of the original WD precludes confinement. To evaluate this option, positron escape in the absence of a magnetic field is calculated for both a Chandrasekhar and a sub-Chandrasekhar explosion model (model W7 and model WD065 of the detonated WD of $0.65 M_{\odot}$). 2) A radially combed-out magnetic field enhances escape in a low-mass WD explosion and in a Chandrasekhar WD explosion (same models and model 2 of the edge-lit detonation of a $0.7 M_{\odot}$ WD). None of the hypotheses combining a Chandrasekhar mass model and enhanced escape can account for a 50% of deposition of the ^{56}Co -decay energy at 200 days. As shown in Fig. 5, the option of lack of a significant magnetic field and a small ejecta mass, as in model WD065, gives a reasonable agreement with the observations. In the absence of a magnetic field, positrons lose their energy according to the interactions undergone along their free trajectories. The sort of calculations done here rescale the γ -ray results to an opacity appropriate for

the processes undergone by the e^+ : $\kappa_e \sim 10 \text{ g}^{-1} \text{ cm}^2$ (Axelrod 1980; Colgate, Petschek, & Kriese 1980). The calculation then reproduces the observed decline rates.

The picture described here of positron transport in the ejecta corresponds to zero confinement or negligible action of the magnetic field. Such condition occurs when the magnetic field intensity of the WD prior to explosion is lower than 10^{3-4}G . Thus, this looks like a plausible explanation for SN 1991bg: *low-mass and weak magnetic field prior to expansion. Lack of confinement but a Chandrasekhar-mass explosion gives a light curve much closer to full-trapping and it departs much later than observed.*

The option of the enhanced escape through radial magnetic fields had to be evaluated by integrating the trajectories of the positrons. Escape occurs in Chandrasekhar-mass explosions at a level lower than observed. Low-mass and a radially combed but strong magnetic field is thus another possible explanation, although less likely from the implications of evolution in time of the magnetic field.

To summarize, the bolometric light curve of SN 1991bg can be well accounted for if positrons are not confined by the post-explosion magnetic field, due to a low initial magnetic field or a radially combed-out magnetic field in low-density ejecta (small mass). The observed light curve seems hard to fit with Chandrasekhar-mass WD explosions, since even for the most favorable configuration of the magnetic field to enhance escape, a Chandrasekhar mass of ejecta would be enough to produce significant deposition of β^+ energy.

5.5. Bolometric light curves and the mass in Type Ibc

The mass of the star at the time of the explosion in Type Ibc is a matter of discussion, and it is linked to the identification of their progenitors. The well observed bolometric light curve of SN 1994I (Richmond et al. 1995) allows us to discuss models for Type Ibc SNe as compared with the observations. The precursors of Type Ibc could be Wolf–Rayet stars, with main sequence masses in the range of 30–40 M_{\odot} . Those stars undergo strong winds and also mass transfer, if they are in binary systems. Mass transfer and winds might produce the loss of the H envelope in the star without removing completely the He envelope. After undergoing gravitational collapse at the end of their evolution, a total ejected mass close to 2 M_{\odot} is expected from this massive progenitor case (Woosley, Langer, & Weaver 1996). In other scenarios, the initial mass of the progenitor is smaller—i.e. in the range of 10–20 M_{\odot} —, and the star ends up its evolution, after having lost both the H envelope and the He mantle, as a bare C+O core. The ejecta mass could be below 1 M_{\odot} . Both γ -ray and energy deposition by positrons should be different in the two cases. Spectral calculations show the need of enhanced mixing in SN 1994I, and in other SNe Ic (Eastman & Woosley 1997; Ruiz–Lapuente 1997). Large–scale mixing, required for SNe Ic, will affect very much the deposition of energy by positrons, and thus the bolometric luminosity. Figure 6 shows the difference that mixing induces in the deposition of γ -rays in Type Ibc models. Mixing enhances as well the escape of energy from positrons. In ejecta with masses lower than 1 M_{\odot} it leads to a departure from the full–trapping curve of ^{56}Co decay. Figure 7 shows the deposition of energy from e^+ and its evolution in time for different models of SNe Ibc and the chaotic configuration of the magnetic field. Model 7A corresponds to the more massive progenitor option mentioned above, and model 7A mixed

has the same ejected mass, but with large-scale mixing (Woosley, Langer, & Weaver 1996; Eastman & Woosley 1996), as required from the spectra. Model CO21 (Nomoto et al. 1996) corresponds to the less massive progenitor, and a mixed version has also been calculated.

It can be seen, that the positron energy is not deposited in the ejecta of exploded C+O stars already at 200 days after explosion. A more massive ejecta than $1 M_{\odot}$ seems to be required to produce effective trapping of the energy from γ -rays and positrons and preclude a fast decline of the luminosity. As shown in Figure 8, such requirement gives a good account of the observed bolometric light curve of SN 1994 I.

6. Positron escape and the Galactic 511 keV line

The positron annihilation radiation towards the Galactic center (Haymes et al. 1975) is believed to originate from two contributions: a time-variable compact source located in the Galactic center and a diffuse component along the Galactic plane. Supernovae have been identified as a likely origin for the diffuse component: positrons escaping from supernovae and annihilating in the surrounding regions would give rise to that emission (Lingenfelter & Ramaty 1989). The width of the diffuse 511 keV radiation places strong constraints on the temperature and density of the region where the annihilation takes place (Ramaty & Mészáros 1981; Guessoum, Ramaty & Lingenfelter 1991; Wallyn et al. 1993). It is found that electron-positron pairs need to lose their energy in a dense medium before annihilating, or the 511 keV would be broadened and blueshifted (Ramaty & Mészáros 1981). Our findings about positron confinement suggest that the SN ejecta are a first site where positron can be confined, as the ejecta evolve into the remnant phase. The way in which the nonthermal

positrons are retained in the increasingly diluted ejecta until they escape to the neighbouring ISM depends on the intensity and configuration of the WD magnetic field prior to explosion, which is determined by the WD evolutionary path. Type Ia supernovae exploding as centrally ignited Chandrasekhar WDs would favor confinement through a chaotic magnetic field, whereas sub-Chandrasekhar edge-lit WDs present an environment more favorable to escape of positrons from their site of origin, although those particles find in the region of interaction between the supernova and the interstellar medium a shield precluding further escape.

7. Conclusions

This work has shown that the bolometric light curves of SNe Ia trace a poorly investigated property of the supernova progenitors: their magnetic field. Through a well tracked departure from the full-trapping curve of ^{56}Co decay, insights on the pre-expansion magnetic field of the star can be obtained. It can be investigated whether the convective turbulence previous to the explosion in accreting WDs succeeds in amplifying the mean intensity of the original magnetic field of the WD by winding up the magnetic field lines. Or whether, on the contrary, the original WD magnetic field prevails without growing significantly before the explosion and its intensity simply decreases as the supernova expands. The consequences of these two extreme hypothesis have appreciable different impacts on the supernova luminosity. It is possible that Chandrasekhar WDs develop a highly tangled magnetic field which would favor a bolometric light curve close to full-trapping of ^{56}Co decay positrons energy. The important phase when this can occur is the period when accretion and gain in mass of the C+O WDs lead to a compression and quasistatic C burning in

the center. A central convective core is developed several thousands years before the explosion. This should be a distinctive signature of C+O accreting WDs precursors of centrally ignited Chandrasekhar explosions. It is not expected to occur in sub-Chandrasekhar WDs ignited through He detonations. In those explosions, the initial magnetic field of the WD would have preserved its initial configuration enhancing the escape of the energy of the positrons.

On the other hand, differences in the distribution of radioactive material in velocity space and in the mass of the exploding WDs give rise as well to different declines in the late-time bolometric luminosity of SNe Ia. A tabulation of typical decline rates resulting from different explosion mechanisms is given to facilitate comparisons with observations. Three different epochs can be considered in the deposition of energy from ^{56}Co : a first phase where γ -ray deposition is sustaining the early ^{56}Co tail. A second phase where the γ -ray contribution is starting to become negligible and β^+ -rays start to provide the luminosity. In this second phase the density of the ejecta (provided that the ejected masses are close to $1.4 M_{\odot}$) is still high enough to ensure the effectivity of positron energy deposition. And a third phase in which the density of the ejecta is not high enough to trap significantly the positron energy and the configuration and intensity of the magnetic field determines the fate of the released energy. A very wide difference in the tails of the bolometric luminosity at this phase could easily be linked to different intensities of the magnetic field previous to the enormous expansion resulting from the explosion. If a wide diversity (larger than 30%) is found even earlier, in the second phase –i.e, as soon as γ -rays become a negligible energy contribution–, since at that time the density of the ejecta should still be high enough to slow down the positrons, the departure points towards an enhanced escape favored by the preserved but

expanded dipole structure of the original B of the WD, and, also to possible low mass of the ejecta in case of a extreme escape occurring as early as in SN 1991bg. A lesser degree of diversity (lower than 10 – 15% in deposition) in the bolometric decline at this intermediate phase could be interpreted as differences in the kinematics and ^{56}Co -distribution in the supernovae.

Our analysis of SN 1972E suggests that full-trapping lasted at least 400–500 days. The Chandrasekhar model W7 accounts well for the overall shape of the bolometric light curve. The decline of the supernova so close to full-trapping and the late departure taking place at about 740 days after explosion indicates that a tangled magnetic field of at least 10^5G had developed in this supernova. In the case of SN 1991bg, the early and large escape of energy suggests a lower B_0 previous to explosion (lower than 10^{3-4}G), or a dipole magnetic field expanded towards a radial structure. Whereas in SN 1972E there is no evidence pointing towards a mass lower than the Chandrasekhar mass, in SN 1991bg even within magnetic field configurations maximally favoring escape, a Chandrasekhar-mass WD would still show larger trapping of radioactive energy than observed. A very good agreement with the observations of SN 1991bg is found if confinement is negligible and the total mass of the ejecta is *a half of a Chandrasekhar mass*.

On the other hand, in determining the evolution of the bolometric luminosity of core-collapse supernovae (coming from massive stars) and their ejected mass, mixing plays a fundamental role. A study of the mixing in each type of core-collapse SN through spectral modeling is needed before deriving any conclusions on the ejected mass and on the amount of ^{56}Ni synthesized in those explosions. The mass of the star at the time of the explosion in Type Ibc is a subject of discussion, even in such well-observed cases as SN 1994 I. Examining

the bolometric light curve of this supernova, and the mixing constraints from the spectra, a better agreement with the more massive progenitor is suggested. The diversity in the bolometric luminosity of Type Ibc can be linked both to mixing and ejected mass differences among the exploded stars giving rise to this supernova class. A longer follow-up of their bolometric light curves will help to determine the trapping of ^{56}Co energy and to clarify the actual mass range of the stars which explode as supernovae of different types.

P.R.L thanks the very stimulating discussions with Wolfgang Hillebrandt in relation to this work, and useful information provided by him, Dave Arnett and Jens Niemeyer on convection in WDs. Thanks go as well to Peter Milne for interesting exchanges on positron transport in supernovae. Financial support for this work has been provided by the Spanish DGICYT.

REFERENCES

- Arnett, W.D. 1969, *Ap&SS*, 5, 180
- Arnett, W.D. 1996, *Supernovae and nucleosynthesis*. Princeton series in astrophysics, Princeton, NJ: Princeton University Press, p. 354
- Axelrod, T. S. 1980, Ph D. Thesis, U. California at Santa Cruz
- Berger, M.J. & Seltzer, S.M. 1964, *Tables of Energy Losses & Ranges of Electrons & Positrons* (Washington, DC: NASA)
- Blumenthal, G.B. & Gould, R. J. 1970, *Rev. Mod. Phys.*, 42, 237
- Bravo, E. , Tornambé, A., Domínguez, I., & Isern, J. 1996, *A & A*, 306, 811
- Chan, K. & Lingenfelter, R. E. 1993, *ApJ*, 403, 614
- Colgate, S. A., Petschek, A.G., & Kriese, J. T., 1980, *ApJ*, 237, L81
- Colgate, S. A. 1990. in *Supernovae*, ed. S. Woosley, (Springer–Verlag, Berlin), 585
- Colgate, S. A., Fryer, C. L., & Hand, K. P. 1997. in *Thermonuclear Supernovae*, ed. P. Ruiz–Lapuente, R. Canal & J. Isern. Kluwer Academic Publishers, 273
- Gould, R.J. 1972, *Physica*, 60, 145
- Guessoum, N., Ramaty, R. & Lingenfelter, R.E. 1991, *ApJ* 378, 170
- Hamuy, M. et al. 1996a, *AJ*, 112, 2438
- Hamuy, M. et al. 1996b, *AJ*, 112, 2408
- Haymes, R.C. et al. 1975, *ApJ*, 201, 593
- Heitler, w. 1954, *The Quantum Theory of Radiation* (3d. ed.; Oxford: Clarendon Press)

- Hernanz, M., Salaris, M., Isern, J. & José, J. 1997, in *Thermonuclear Supernovae*, ed. P. Ruiz–Lapuente, R. Canal & J. Isern. Kluwer Academic Publishers, 167
- Khokhlov, A. A& A, L25 (1991)
- Kirshner, R. P. 1997, private communication
- Kirshner, R.P & Oke, J.B. 1975, *ApJ*, 200, 574
- Kraichnan, R. H. 1976, *J.Fluid. Mech*, 77, 753
- Liebert, J. 1995 in *Proceedings of the Cape Workshop on Magnetic Cataclysmic Variables*. ASP. Conference Series, Vol. 85. D. A. H. Buckley and B. Warner, eds.
- Lingenfelter, R.E. & Ramaty, R. 1989, *ApJ*, 343, 686
- Livne, E. & Arnett, D. 1995, *ApJ* 452, 62
- Niemeyer, J. C. & Hillebrandt, W. 1995, *ApJ*, 452, 769
- Nomoto, K. 1982. *ApJ* 257, 780
- Nomoto, K., Thielemann, F.–K. & Yokoi, K. 1984, *ApJ* 286, 644
- Nomoto, K. 1995 (private communication)
- Nomoto, K., Iwamoto, K., Young, T. R., Nakasato, N. & Suzuki, T. 1997. in *Thermonuclear Supernovae*, ed. P. Ruiz–Lapuente, R. Canal, & J. Isern. Kluwer Academic Publishers, 839
- Porter, A. C., Dickinson, M., Stanford, S. A., Lada, E. A., Fuller, G. A., Myers, P.C. 1992, *BAAS*, 181, 7607
- Ramaty, R. & Mészáros, P. 1981. *ApJ*, 250, 384
- Richmond, M. W., Van Dyk, S.D., Ho, W., Peng, C., Paik, Y., Treffers, R. R., & Filippenko, A. V. 1996, *AJ*, 111, 327

- Riess, A.G., Press, W.H., & Kirshner, R.P. 1996, ApJ 473, 88
- Roy, R.R. & Reed, R.D. 1968, Interactions of Photons and Leptons with Matter
(New York: Academic)
- Ruiz-Lapuente, P. et al. 1993, Nature, 365, 728
- Ruiz-Lapuente, P. 1997 (in preparation)
- Sandage, A., Saha, A., Tammann, G. A., Labhardt, L., Schwengeler, H.,
Panagia, N., & Macchetto, F. D. 1994. ApJ 423, L13
- Segré, E. 1977, Nuclei and Particles (New York: Benjamin / Cummings)
- Suntzeff, N. B. (1996). in IAU Colloq. 145, Supernovae and Supernova
Remnants, ed. R. McCray & Z. W. Li (Cambridge, Cambridge University
Press), Cambridge, p. 41
- Sutherland, P. G. & Wheeler, J. C. 1984. ApJ 280, 282
- Swartz, D.A., Sutherland, P. G. & Harkness, R.P. 1995. ApJ 446, 766
- Turatto, M., Benetti, S., Cappellaro, E., Danziger, I.J., Della Valle, M., Gouiffes
C., Mazzali, P. A., Patat, F. 1996, MNRAS, 283, 1
- Wallyn, P., et al. y 1993, ApJ 403, 621
- Woosley, S. E. 1990, in Supernovae, ed. A. Petschek, (Springer-Verlag, Berlin),
182
- Woosley, S. E. & Weaver, T. A. 1994, ApJ, 423, 371
- Woosley, S. E. 1997, in Thermonuclear Supernovae, ed. P. Ruiz-Lapuente, R.
Canal, & J. Isern. Kluwer Academic Publishers, 313

Table 1: Typical values for the stopping distance and the fraction of the envelope traveled by e^+ of various energies by ionization

	1 keV	10 keV	100 keV	1 MeV
W7 $d_e(300)$	5.2×10^{11}	2.3×10^{13}	1.2×10^{15}	2.8×10^{16}
$\xi(100)$	1.0×10^{-6}	4.4×10^{-5}	2.2×10^{-3}	0.05
$\xi(300)$	9.1×10^{-6}	4.4×10^{-4}	0.02	0.48
LA95M2 $d_e(300)$	1.1×10^{12}	4.9×10^{13}	2.5×10^{15}	5.9×10^{16}
$\xi(100)$	1.6×10^{-6}	6.9×10^{-5}	3.3×10^{-3}	0.08
$\xi(300)$	1.4×10^{-5}	6.2×10^{-4}	0.03	0.75

d_e : stopping distance (in cm)

$$\xi = d_e/R_{env}$$

Table 2: Models for Type Ia ¹

	W7	WPD1	LA95M2	LA95M6	WD065	NIDD
$Mass (M_\odot)$	1.38	1.38	0.7	0.96	0.65	1.07
$Mass \ ^{56}Ni (M_\odot)$	0.63	0.1	0.14	0.65	0.07	0.97
$E_{kin} (10^{51}erg)$	1.3	1.1	0.66	1.33	0.57	1.33

¹Models are: deflagration model W7 of Nomoto, Thielemann & Yokoi (1984); pulsating delayed detonation model WPD1 of Woosley (1997); He–detonation of a 0.7 M_\odot WD (model 2 by Livne & Arnett 1995) and of a 0.96 M_\odot WD (model 6 by Livne & Arnett 1995), a He–detonation of a 1.1 M_\odot WD (Nomoto 1995, here called NIDD), and a bare C+O detonation of a 0.65 M_\odot WD (model WD065 by Ruiz–Lapuente et al. 1993).

Table 3: Declines in absolute magnitude in the e^+ confinement regime

	$\Delta_{m_\gamma}^{100}$	M_{bol}^{100}	$\Delta_{m_{1\beta}}$	$\Delta_{m_{2\beta}}$	M_{bol}^{200}
W7	0.021	-16.	0.013	0.010	-13.9
WPD1	0.022	-14.3	0.013	0.010	-12.11
LA95M2	0.009	-13.6	0.012	0.010	-11.8
LA95M6	0.009	-15.1	0.012	0.011	-13.4
WD065	0.017	-12.4	0.012	0.011	-10.7
NIDD	0.0125	-14.6	0.011	0.011	-13.4

The models are described in Table 2.

Table 4: Deposition of e^+ for different models¹ in the confinement regime

	W7	WPD1	LA95M2	LA95M6	WD065	NIDD
D_β (300d)	100.	95.0	97.8	89.6	100	84.7
D_β (350d)	100.	95.0	95.8	87.2	100	78.6

The models are described in Table 2.

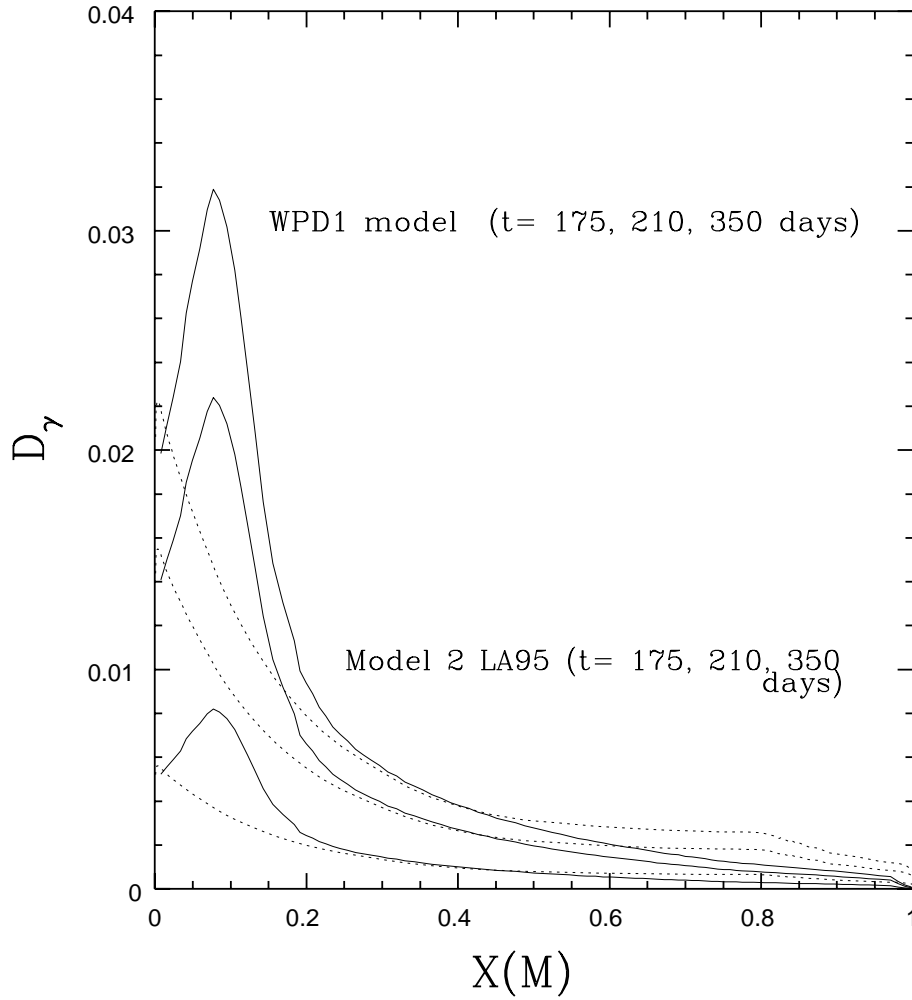


Fig. 1.— Deposition of γ -rays for two alternative models for subluminous SNe Ia: the dashed line displays the deposition function of a sub-Chandrasekhar edge-lit detonation of a $0.7 M_{\odot}$ C+O WD (model 2 by Livne & Arnett 1995), and the solid lines draws the same function for a pulsating delayed detonation model in a Chandrasekhar C+O WD (model WPD1 by Woosley). The deposition profile is calculated at different times after the explosion.

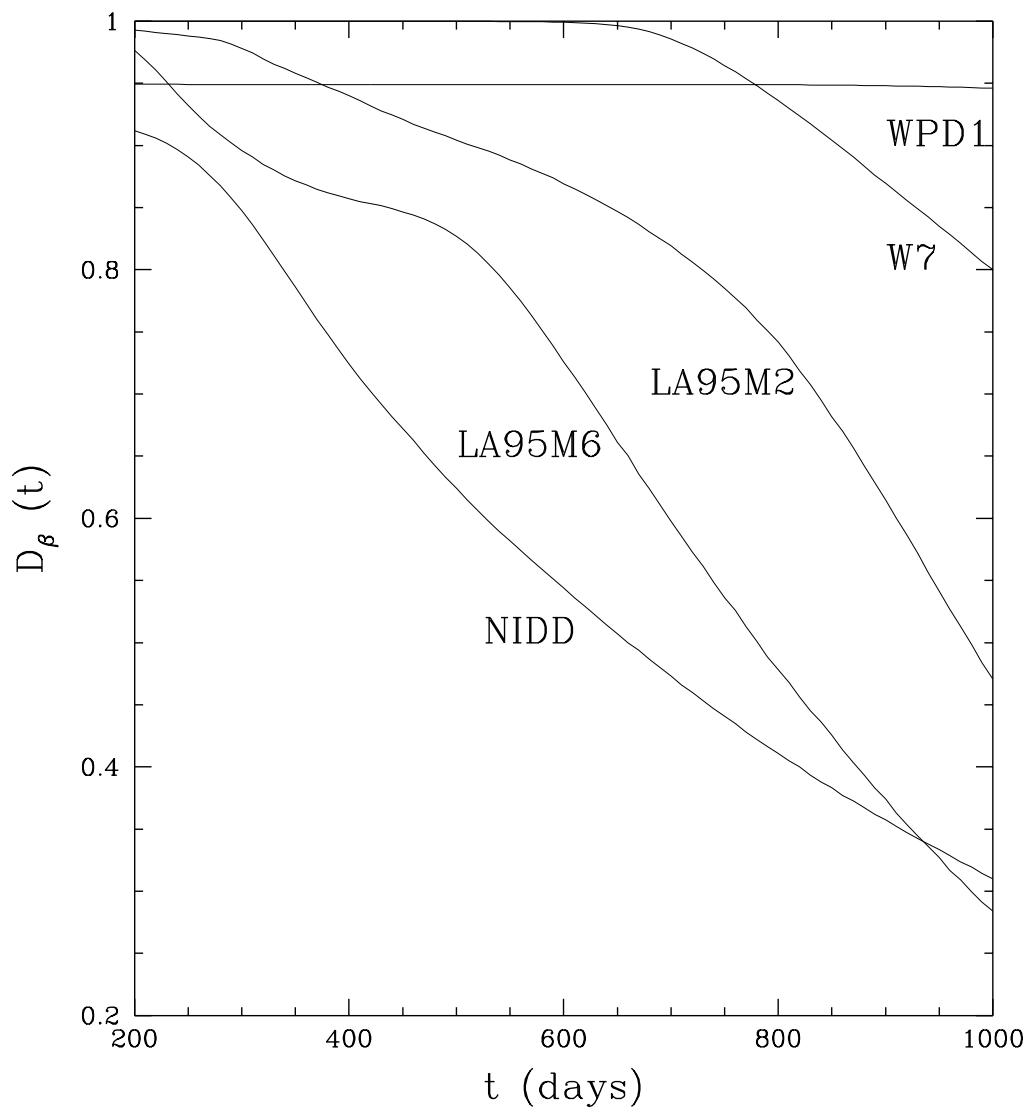


Fig. 2.— Deposition of energy from e^+ for various SNe Ia models. Models are as in Table 1: deflagration model W7 of Nomoto, Thielemann & Yokoi(1984); pulsating delayed detonation model WPD1 of Woosley (1997); He–detonation of a $0.7 M_\odot$ WD (model 2 by Livne & Arnett 1995, i.e LA95M2) and of a $0.96 M_\odot$ WD (model 6 by Livne & Arnett 1995, i.e LA95M6), a He–detonation of a $1.1 M_\odot$ WD (Nomoto 1995, here called NIDD).

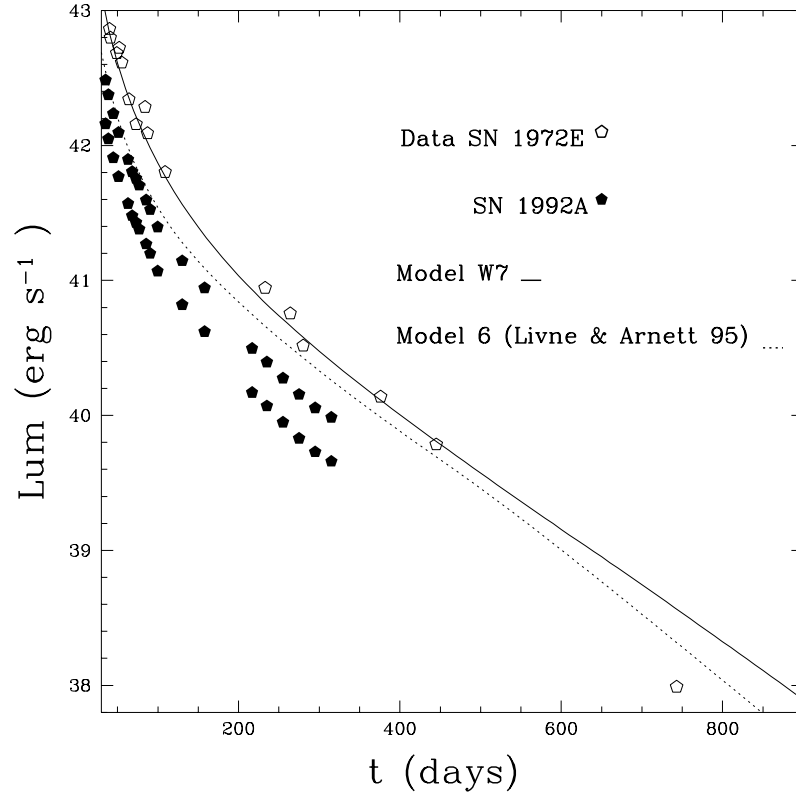


Fig. 3.— Bolometric light curves for the various models compared with the data for SN 1972E (Kirsner & Oke 1975) and the bolometric data for SN 1992A (Suntzeff 1996) shifted in scale of distance ($d=16.5$ and $d=22$ Mpc for NGC 1380). Model W7 by Nomoto, Thielemann & Yokoi(1984) is a deflagration of a Chandrasekhar–mass WD. Model 6 by Livne & Arnett (1995) is a He–detonation of a $0.96 M_{\odot}$ WD.

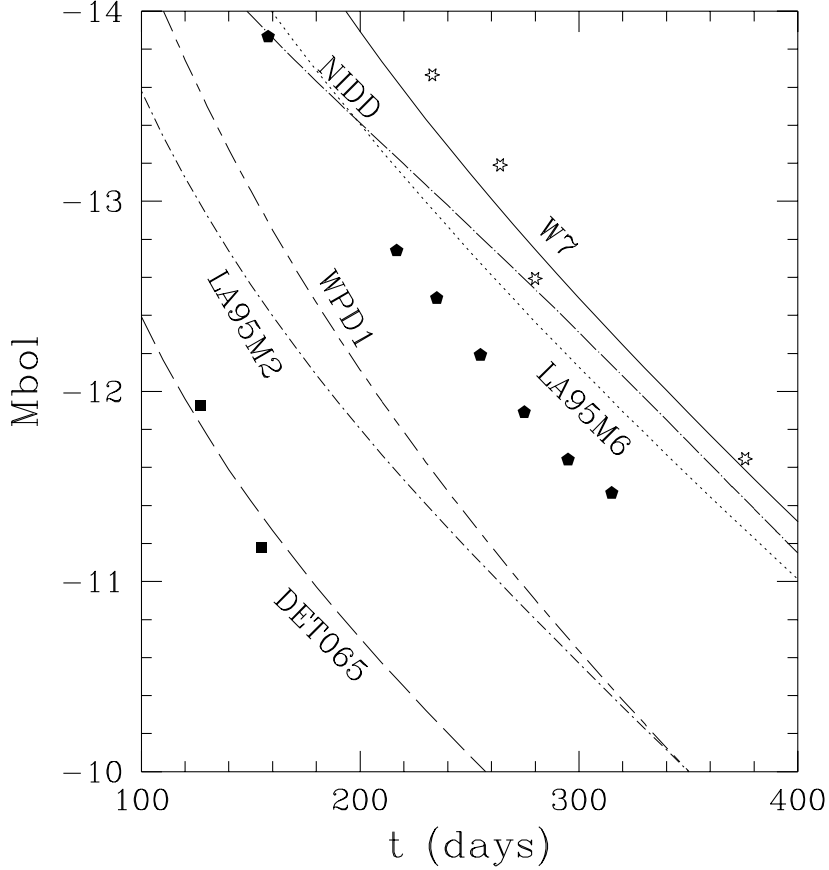


Fig. 4.— Bolometric magnitude–decline for models. Data for SN 1972E (starred symbols), SN 1992A (pentagonal symbols) and SN 1991bg (square symbols) are shown for comparison. The models predictions are displayed by different labeled lines. Model W7 by Nomoto, Thielemann & Yokoi(1984) is a deflagration of a Chandrasekhar–mass WD. Model WPD1 by Woosley (1997) is a pulsating delayed detonation of a Chandrasekhar WD. The model labeled LA95M6 is model 6 by Livne & Arnett (1995), a He–detonation of a $0.96 M_{\odot}$ WD. The model labeled LA95M2 is model 2 by Livne & Arnett (1995), a He–detonation of a $0.7 M_{\odot}$ WD. The model labeled NIDD is a He–detonation of a $1.1 M_{\odot}$ WD as calculated by Nomoto (1995), and model DET065 is a bare detonation of a C+O WD of $0.65 M_{\odot}$ (Ruiz–Lapuente et al. 1993). See details in Table 2.

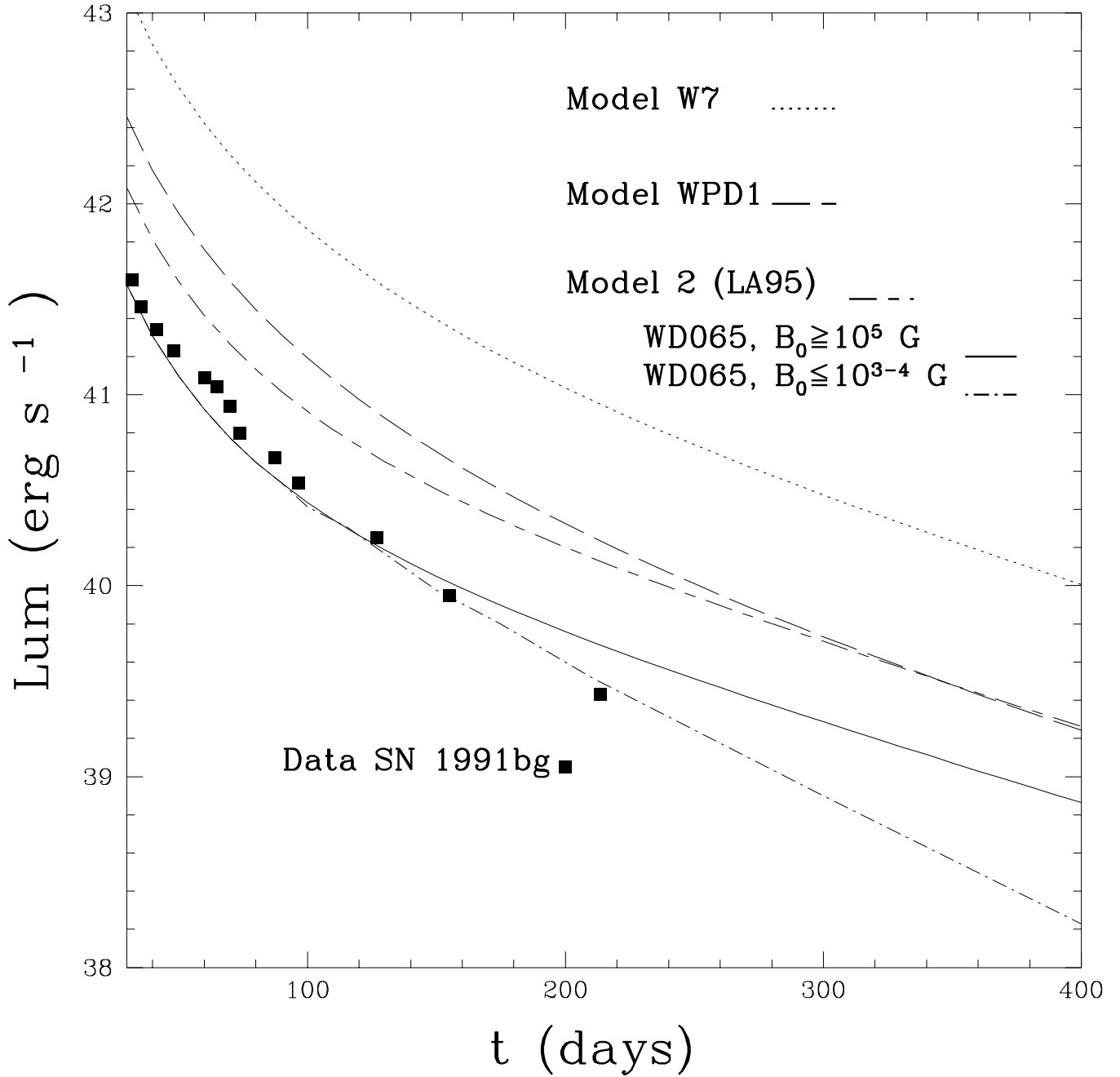


Fig. 5.— Bolometric light curves for various models proposed for subluminous SNe Ia compared with SN 1991bg (Turatto et al. 1995).

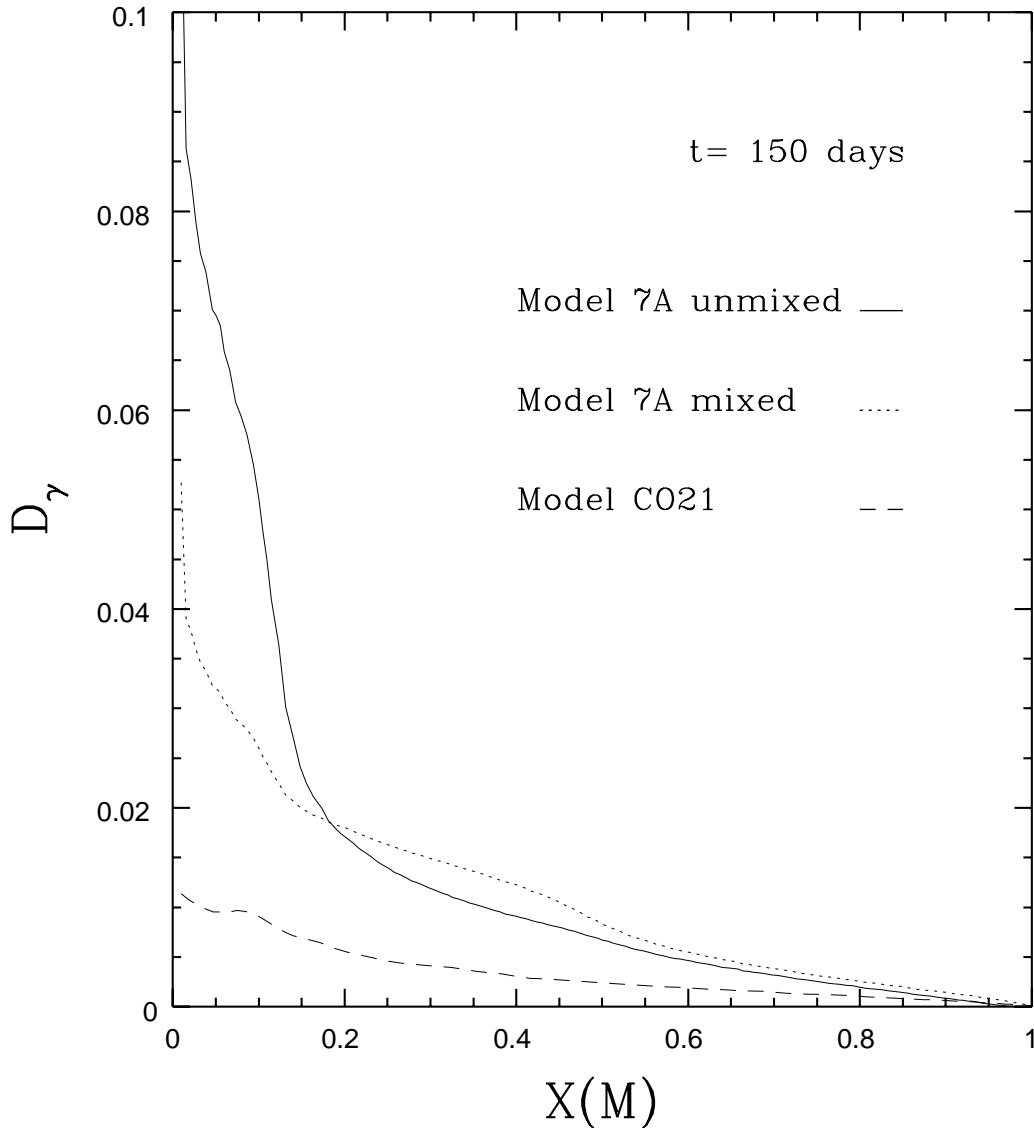


Fig. 6.— Deposition of γ -rays for various models. Model 7A corresponds to the 30–40 M_{\odot} main sequence Wolf–Rayet progenitor for SNe Ibc by Woosley, Langer, & Weaver 1996. Model 7A mixed is a mixed version of Model 7A, which reproduces much better the spectra (Eastman & Woosley 1997; Ruiz–Lapuente 1997). Model CO21 corresponds to the less massive candidate to SNIbc of initial mass in the range 10–20 M_{\odot} which ends up as a C+O star before the explosion (Nomoto et al. 1996).

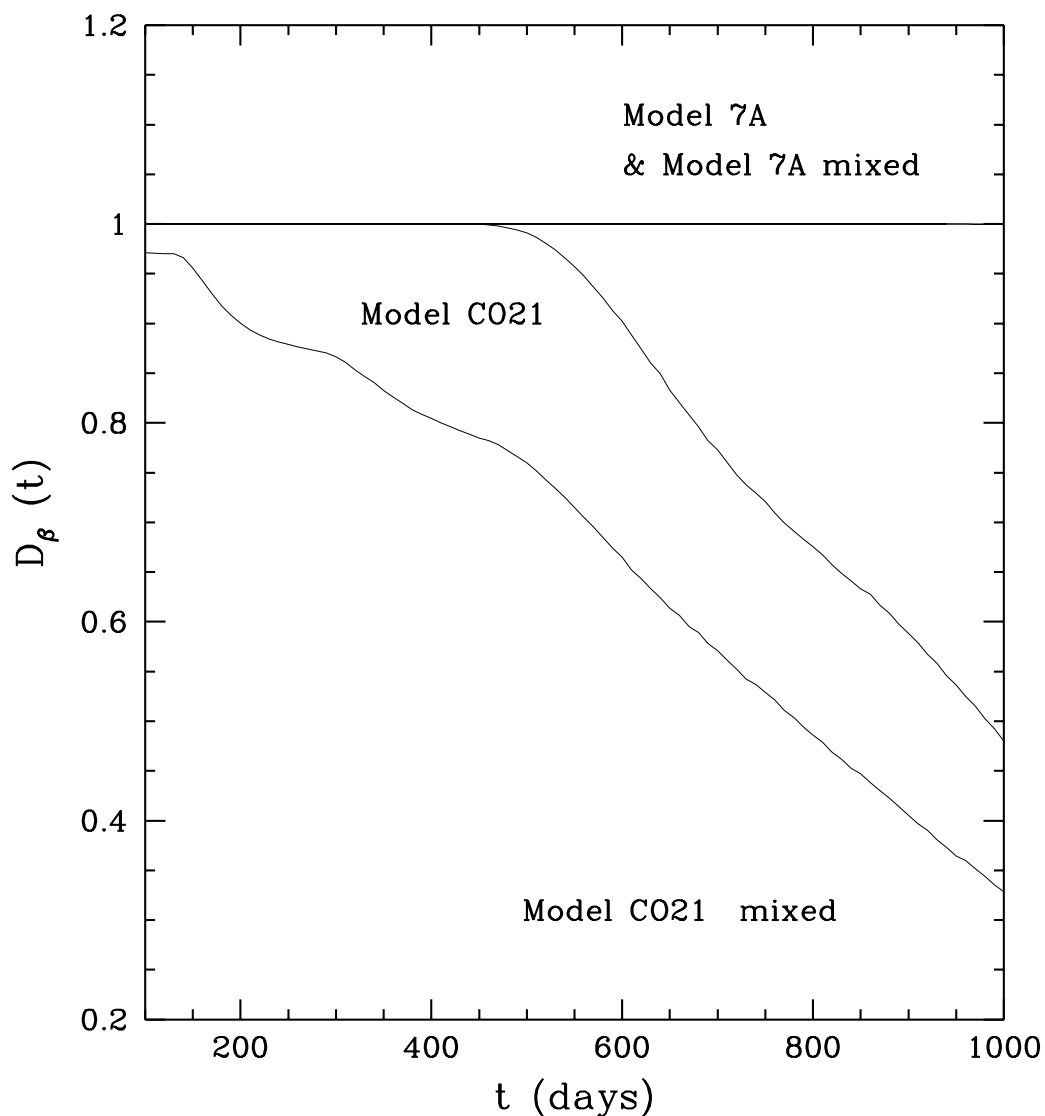


Fig. 7.— Deposition of energy from e^+ for various models. Model 7A corresponds to the 30–40 M_{\odot} main sequence Wolf–Rayet progenitor for SNe Ibc by Woosley, Langer, & Weaver 1996. Model 7A mixed is a mixed version of Model 7A. Model CO21 corresponds to the less massive candidate to SNIbc of initial mass in the range 10–20 M_{\odot} which ends up as a C+O star before the explosion (Nomoto et al. 1996). Model CO21 mixed is a mixed version of Model CO21. Mixing is needed to reproduce the spectra.

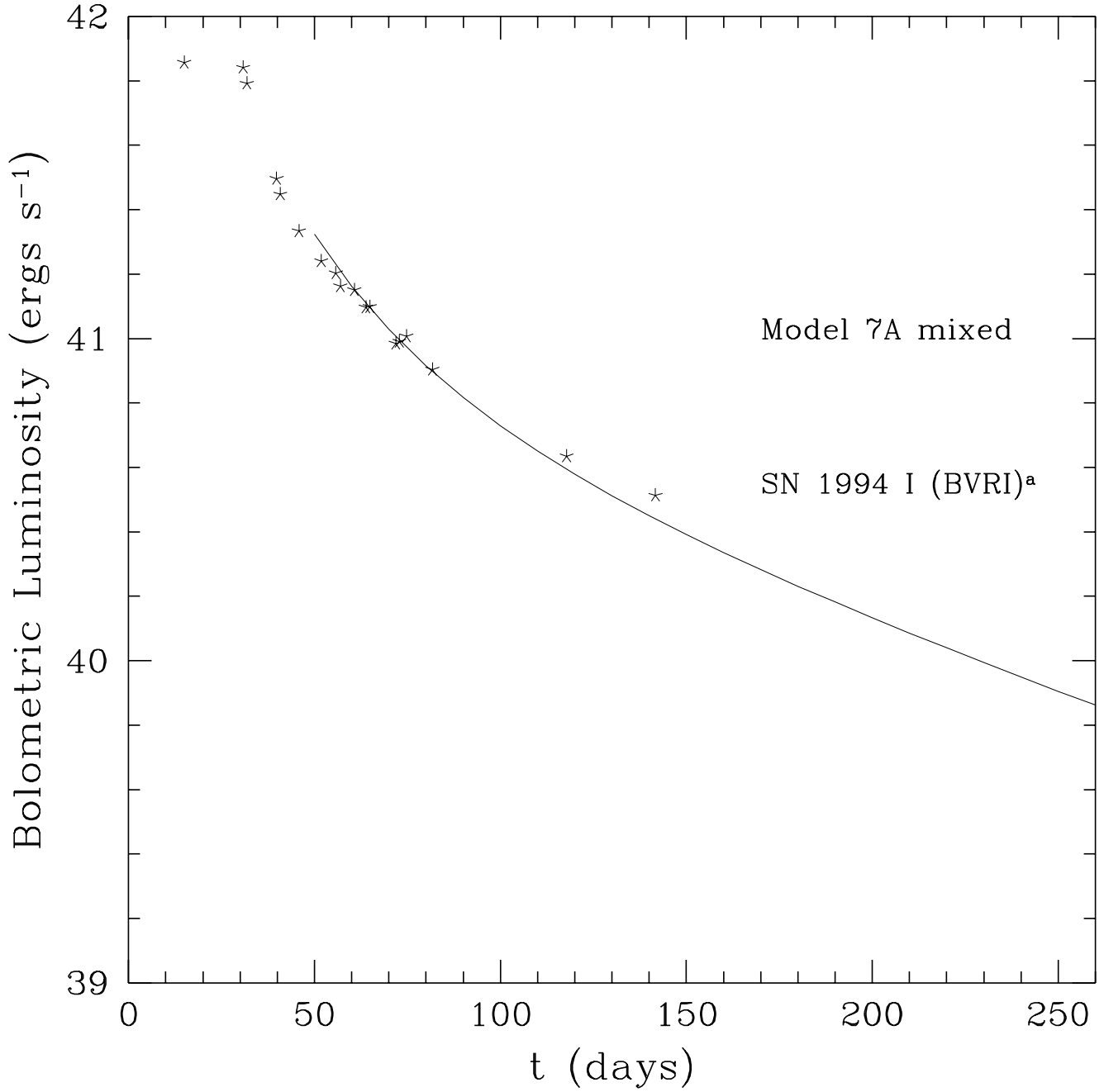


Fig. 8.— Light curve of Model 7a mixed compared with the bolometric of SN 1994I by Richmond et al. (1996) taking as SN reddening $E(B-V)=0.45$.